

SPHERE / ZIMPOL: Characterization of the FLC polarization modulator

Andreas Bazzon^a, Daniel Gisler^a, Ronald Roelfsema^b, Hans M. Schmid^a, Johan Pragt^b, Eddy Elswijk^b, Menno de Haan^b, Mark Downing^c, Bernardo Salasnich^d, Alexey Pavlov^e, Jean-Luc Beuzit^f, Kjetil Dohlen^g, David Mouillet^f, Francois Wildi^h

^aETH Zurich, Institute of Astronomy, Wolfgang-Pauli-Str. 27, 8093 Zurich, Switzerland;

^bNOVA Optical-Infrared Group at ASTRON, 7991 PD, Dwingeloo, The Netherlands;

^cESO, Karl-Schwarzschild-Str. 2, 85748 Garching, Germany;

^dINAF, Osservatorio Astronomico di Padova, Vicolo dell'Osservatorio 5, 35122 Padova, Italy;

^eMax-Planck-Institut für Astronomie, Königstuhl 17, 69117 Heidelberg, Germany;

^fUJF-Grenoble, Inst. de Planétologie et d'Astrophys. de Grenoble (IPAG), Grenoble, 38041, France;

^gLAM, Observatoire de Marseille, 38 rue Frédéric Joliot-Curie, 13388 Marseille, France;

^hObservatoire Astronomique de l'Université de Geneve, 1290 Sauverny, Switzerland

ABSTRACT

ZIMPOL is an imaging polarimeter for the high-contrast SPHERE/VLT “planet finder” instrument using fast polarization modulation and demodulating CCD detectors. The polarimetric performance of the ZIMPOL instrument depends on the polarimetric alignment and quality of the polarization components. This paper gives an overview on the polarimetric concept and the calibration plan of ZIMPOL. We discuss in particular the alignment of the polarimetric calibration components and the polarimetric properties of the ferro-electric liquid crystal (FLC) modulator package used in ZIMPOL. Our measurements demonstrate the good broad-band performance of the modulator. Faint targets, like extra-solar planets, require mainly a high polarimetric efficiency while for detailed studies of bright targets a good characterization of the modulator package is essential. Therefore we quantify in detail the wavelength dependence of the polarimetric efficiency and the cross-talk effects which have to be taken into account in the calibration and data reduction process of high S/N measurements.

Keywords: VLT, high-contrast imaging, polarimetry, CCD, exoplanets, polarization modulator

1. INTRODUCTION

The ESO VLT planet finder instrument SPHERE (Spectro-Polarimetric High contrast Exoplanet REsearch) will become in 2013 one of the most sensitive instruments for high contrast imaging of extra-solar planets and the circumstellar material around bright stars. SPHERE consists of a high-contrast extreme-AO system, different coronagraphs and state of the art imagers, spectrographs and polarimeters for the 0.5 μm to 2.2 μm wavelength range^[1,2].

One of the main challenges for the direct detection of extrasolar planets consists in the detection of a tiny planet signal at very small angular separations of about 0.1-0.4 arcsec to its host star while simultaneously grappling with the large intensity contrast of 10^{-4} for young luminous planets down to 10^{-8} for old reflecting planets.

Light reflected from planetary atmospheres is generally polarized. This property can be used to distinguish polarimetrically the very faint signal of the planet from the unpolarized light of the parent star. Based on this idea we built a fast modulation-demodulation polarimeter which combines high contrast imaging of SPHERE with high precision polarimetry of ZIMPOL. The SPHERE/ZIMPOL system is optimized for the search of reflected polarized light from old giant planets around nearby ($d < 10$ pc) stars in the wavelength range between 520 and 900 nm^[3]. SPHERE/ZIMPOL

can also be used in imaging mode with the diffraction limited resolution of 15-20 mas provided by the 8.2 m VLT unit telescope and the SPHERE extreme AO system. This provides many other science opportunities besides exoplanet research.

This work describes in Chapter 2 the fast modulation-demodulation technique implemented in ZIMPOL and in Chapter 3 the polarimetric concept of SPHERE/ZIMPOL. Chapter 4 and 5 are dedicated to the polarimetric calibration of SPHERE/ZIMPOL and the calibration components and their alignment. In Chapter 6 we describe our calibration measurements of the modulator package and in Chapter 7 we present our conclusions.

2. THE ZIMPOL PRINCIPLE

The ZIMPOL principle (Zurich IMaging POLarimeter) is based on a fast modulation-demodulation technique using charge-shifting on a masked CCD detector. It was originally built for solar observations and proved to be a very powerful technique to detect very weak polarization signals^[4,5,6]. It routinely achieved a sensitivity of better than 10^{-5} and it has been demonstrated that the same performance will also be achievable for a planet finder instrument^[7,8].

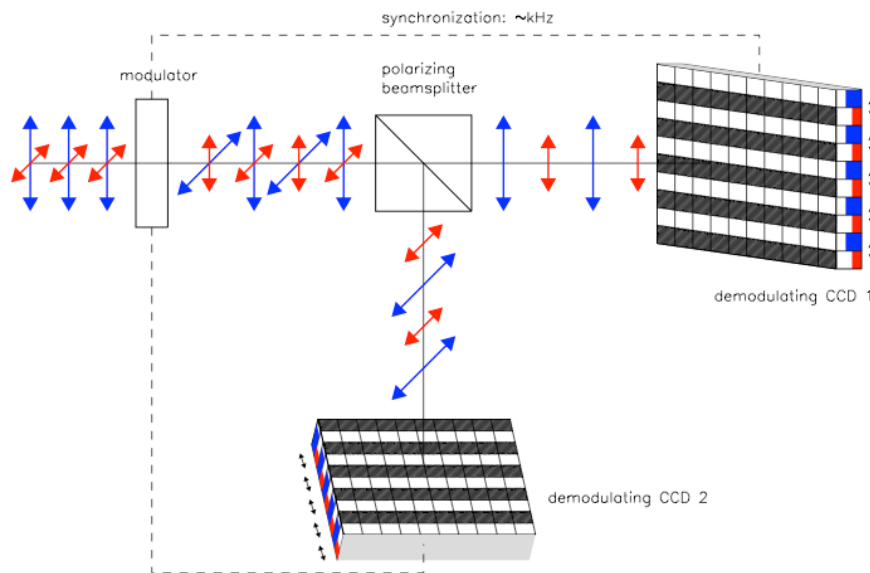


Figure 1 A schematic illustration of the ZIMPOL principle. Note that one CCD is sufficient for a fully functional imaging polarimeter. Explanations are given in the text.

In ZIMPOL an incoming polarization signal is transformed into a temporally modulated intensity signal by a modulating electro-optical retarder followed by a linear polarizer. The modulated signal is stored in two image planes by specially masked CCD detectors and the polarization can be determined by a differential intensity measurement. The masked CCDs consist of alternating open and covered rows and the charges corresponding to the two modulation states are shifted in synchrony with the polarization modulator forwards and backwards behind this mask for real time demodulation. To minimize the efficiency loss due to the stripe mask the ZIMPOL CCD is further equipped with a microlens array which focuses the incoming light to the narrow opening slits of the mask.

Since the sensor does not have to be read out between the single modulation states the frequency of modulation can be faster than the seeing variations and the images for the opposite polarization states are recorded practically simultaneously. Because the two modulation states are sampled by the same pixels on the CCD differential aberrations are minimized and there is no dependence on the single pixel sensitivity. Furthermore, by shifting the demodulation phase by half a cycle between consecutive pairs of frames charge transfer effects of individual pixels are also compensated^[7].

The stripe masking and the fast charge shifting operational modes with cycle frequencies around 1 kHz clearly distinguish the system from more common applications of CCD detectors. Hence, charge transfer inefficiency, frame transfer smearing, charge pockets, charge diffusion from open to covered pixel rows and other detector effects need to be under control. For a description of the CCD operation and performance refer to Schmid et al. (2012)^[9].

3. SPHERE / ZIMPOL POLARIMETRIC CONCEPT

SPHERE is a large and complex instrument which will be mounted on the Nasmyth platform of one of the 8.2 m VLT unit telescopes. This implies that there will be many optical components which introduce instrumental polarization effects: the inclined telescope mirror M3, a field derotator and a complicated common path instrument (CPI) consisting of many mirrors and additional correction optics. Hence, for the polarimetric measurement it would be preferable to have the polarization analysis as early in the beam as possible. But this would have a very disturbing impact on the extreme AO-system, and the other subsystems. Therefore, the ZIMPOL modulator is placed behind many other optical components. This requires a significant effort to control and calibrate the instrument polarization. This chapter gives an overview of the polarimetric concept of SPHERE/ZIMPOL while the basic polarimetric calibration approach is described in the next chapter.

The block diagram in Figure 2 gives a “polarimetric” overview of ZIMPOL and the SPHERE-CPI system. The latter includes a derotator, the tip-tilt and deformable mirrors from the AO system, beam-splitters, an atmospheric dispersion corrector, relay optics, and a coronagraph system. Polarimetrically important components are plotted in color.

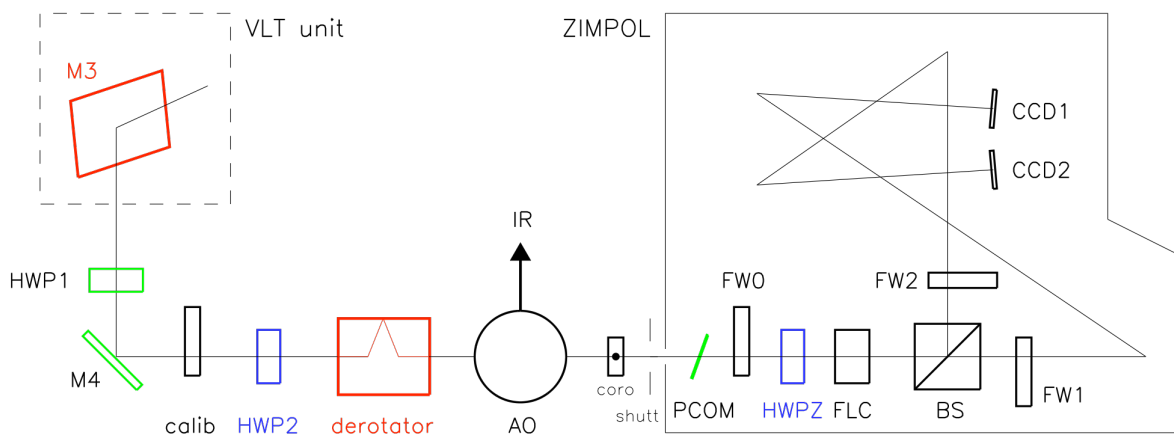


Figure 2. Overview of the SPHERE/ZIMPOL optical path. Indicated in red are the components that introduce substantial instrumental polarization (>1%). The components in blue are used to rotate the Stokes vector into the derotator system and back into the ZIMPOL system respectively. Green indicates components which compensate the instrumental polarization from preceding components.

3.1 ZIMPOL in SPHERE

ZIMPOL measures the polarization signal at the position of the analyzing polarimetric components, which are the modulator and the beam-splitter. One arm of ZIMPOL provides a full polarimetric measurement. The second arm measures the same polarimetric information (if the same filters are used in FW1 and FW2) and it ensures that no light is wasted. The two filter wheels provide the possibility to take polarimetry in two different bands simultaneously. The common filter wheel FWO contains polarimetric calibration components and additional filters for imaging.

ZIMPOL can only measure the linear polarization component parallel I_0 or perpendicular I_{90} to the optical bench. Other polarization position angles must be selected by a rotating half wave-plate located in front of ZIMPOL. This role is taken

by HWP2 in the common path and if the derotator is offset from a vertical position then another half-wave plate within ZIMPOL (HWPZ) must be used (see below).

ZIMPOL has an instantaneous field of view of 3.5 arcsec^2 and will be operating in the wavelength range 520-900 nm. All optical components including the FLC are designed to be achromatic over this wavelength range.

3.2 Compensation of the telescope polarization

The VLT folding mirror M3 reflects the light coming from the secondary mirror onto the Nasmyth platform. This 45° deflection introduces about 3-5% instrumental polarization for wavelengths between 500 and 900 nm. Moreover, because M3 is rotating with the zenith angle the introduced polarization direction is changing with time.

This instrumental polarization can be compensated with two steps. First, the rotation of the polarization vector is stabilized by introducing a half-wave plate (HWP1) which is rotating with half the angular speed of M3. Then the polarization offset produced by M3 is compensated by a second mirror M4 with the same optical properties which stands in a so-called crossed configuration relative to M3. This means that the light which is reflected at M3 by 90° in a vertical reflection plane is followed by a second 90° deflection at M4 but with a horizontal reflection plane so that the polarization effects introduced by M3 are fully compensated by M4 if the mirror coating properties are identical^[10].

3.3 The derotator polarization and the role of HWP2 and HWPZ

SPHERE uses a 3-mirror derotator for field or pupil stabilization, where two mirrors introduce large beam deflections with angles $> 90^\circ$ causing again substantial instrumental polarization and polarization cross-talks between circular and linear polarization states. The cross-talks can be avoided by rotating the linear polarization direction to be measured by ZIMPOL into the orientation of the derotator, which is either parallel or perpendicular to the reflection planes. This is achieved by the CPI half-wave plate (HWP2) in front of the derotator. HWP2 takes into account the selected polarization angle for the measurement, the target polarization rotation which depends on parallactic angle, telescope altitude, and the polarimetric rotation introduced by HWP1. The polarization offset introduced by the derotator is compensated by a co-rotating polarization compensator plate within ZIMPOL. Then as last step one needs to rotate the polarization direction to be measured, which has still the orientation of the derotator, into the fixed ZIMPOL analyzing system which is parallel or perpendicular to the polarizing beam-splitter. Therefore, another co-rotating $\lambda/2$ retarder (HWPZ) is needed to rotate the Stokes vector selected by HWP2 back into the ZIMPOL system.

For different science applications three different types of HWP2-derotator-HWPZ observing modes are offered by SPHERE/ZIMPOL:

- **P1: No field derotation**

For bright targets the integration times can be short enough for observations without image derotation because the rotational smearing of the signal on the detector can be neglected. The rotator is fixed in vertical position. This has the advantage that all components are fixed except for HWP1 which needs to correct for the altitude dependence of the M3 polarization, and HWP2, which rotates the polarization position angle correctly into the orientation of the derotator and the ZIMPOL system. This mode will provide the highest precision polarimetry, best suited for the search of planets around bright stars because nothing moves after HWP2.

- **P2: Active field derotation**

This mode is suited for long integration of fainter targets. Field derotation is activated and the polarization vector is rotated by HWP2 into the rotating derotator system and rotated back by HWPZ into the ZIMPOL system. Therefore, the field is fixed but the instrument polarization can have some drift due to the rotating components.

- **P3: Pseudo-derotation**

This is a combination of P1 and P2 and is best suited for targets which need field derotation to avoid rotational smearing but still need a high polarimetric accuracy. The field is fixed like for the P2 mode for a 5-10 minute observation with the derotator close to the vertical position as in P1 mode. After about 10 minutes the derotator is reset so that it can again derotate for some time near the vertical derotator position. In this way the instrument configuration is always close to the polarimetrically well characterized P1 configuration.

3.4 Polarization switch and the compensation of the CPI polarization

Polarimetric switching is a very useful technique to compensate or calibrate instrumental effects between the switching position and the analyzing system (i.e. the modulator package). A HWP2 switch, a rotation of HWP2 by 45° , introduces a sign change (a 90° rotation of the polarization direction) for the polarization in front of the switch position whereas the sign of the instrumental polarization after the switch remains unchanged. Therefore, a subtraction of two observations taken with HWP2 switched will sustain the polarimetric signal from the sky (and telescope) while the instrumental polarization introduced downstream from HWP2 is canceled. This concept is illustrated in Figure 3.

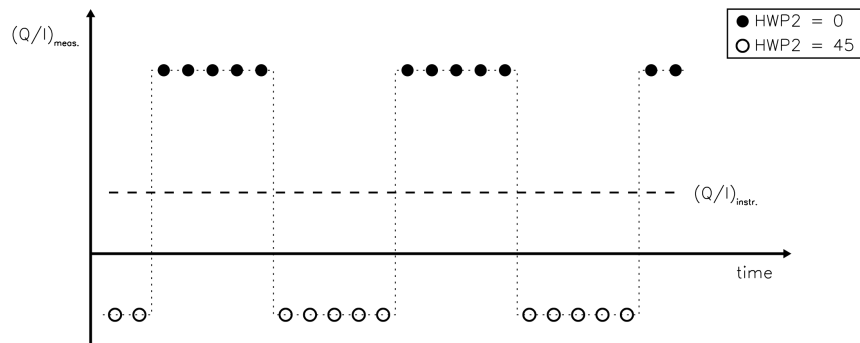


Figure 3 Polarimetric switching to compensate and correct for instrumental polarization: The sign of the polarization in front of the switch (i.e. the planet signal and the sky polarization) is reversed while the instrumental polarization after the switch remains constant.

In SPHERE/ZIMPOL the switching is implemented by a 45° rotation of HWP2 relative to the actual orientation. It is an essential part of the calibration of the instrumental CPI polarization which includes the derotator, 9 small-angle ($< 5.5^\circ$) reflections with minor polarimetric impact, and a coronagraph system. Furthermore, the switch is important to remove a 10^{-4} effect caused by the modulator referred to as the “bumpy background effect”^[11].

Finally, except for some small drifts due to the rotating components of CPI the instrumental polarization of CPI is expected to be more or less constant over a long period of time (at least one observing night) and it can be measured by the HWP2-switch. Therefore, it is compensated at the entrance of ZIMPOL by the polarization compensator (PCOM), i.e. a tilted glass plate co-rotating with the derotator.

4. POLARIMETRIC CALIBRATION OF SPHERE / ZIMPOL

The polarimetric calibration of SPHERE/ZIMPOL is based on a step-by-step approach and can be divided into four parts. Starting with the detector calibration, the calibration of each instrument part further upstream will depend on the calibration of the following components further downstream. Except for the telescope calibration which will use on-sky sources the different instrument sections make use of internal light sources and built-in calibration optics which are described in the next chapter.

- **Detector calibration:**

The stripe masking and the fast charge shifting operational modes of the ZIMPOL detectors clearly distinguish the system from more common applications of CCD detectors. Hence, the demodulation efficiency must be calibrated and charge transfer effects (e.g. charge traps, frame transfer smearing, etc.) must be corrected in the data reduction process. A description of the CCD operation and calibration and an assessment of the performance is given in Schmid et al. (2012)^[9].

- Calibration of the modulator package:**
 The modulator package consists of HWPZ which rotates (if necessary) the incoming polarization direction from the derotator into the ZIMPOL analyzing system consisting of modulator and polarizing beam-splitter. All polarimetric components are designed for a broad wavelength range and they show therefore a wavelength dependence in their efficiency and polarization cross-talks which are described in Chapter 6.
- CPI offset and cross-talks:**
 The common path includes an own set of polarization calibration components located in front of HWP2 which are operated in a similar way as for ZIMPOL. A detailed description is out of the scope of this document but some comments are given in Chapter 3.
- Telescope zero-point, offset and cross-talks:**
 In Section 3.2 we described the compensation of the telescope polarization by the combination M3-HWP1-M4. However, it is expected that a low level of instrumental polarization $< 1\%$ and some polarization cross-talks will still be present. These remaining effects will be quantified by on sky calibrations of unpolarized and polarized standard stars.

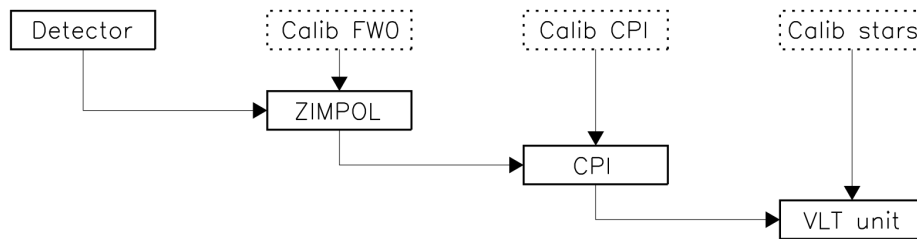


Figure 4 Polarimetric calibration chain for SPHERE/ZIMPOL. Starting with the polarimetric detector calibration (demodulation efficiency and charge transfer effects) each part further upstream will depend on the calibration of the following parts downstream.

5. ZIMPOL CALIBRATION OPTICS

ZIMPOL is equipped with its own set of polarization calibration components located in filter wheel FW0 in front of HWPZ (see Figure 2) consisting of a linear polarizer, a quarter-wave plate, and a circular polarizer. In addition one can use a combination of these components with the rotatable half-wave plate of ZIMPOL (HWPZ). However note that the half-wave plate also needs to be calibrated itself. The reference position angle for the polarimetric system of ZIMPOL is given by the polarizing beam-splitter. The polarimetric properties of the beam-splitter, of the ZIMPOL calibration components, and of HWPZ and the alignment of the zero-points of their polarimetric axis is described in the following sections.

5.1 Polarimetric properties of the ZIMPOL beam-splitter

The achromatic polarizing beam-splitter cube used in ZIMPOL is optimized for the wavelength range of 500-900nm and the transmitted beam is essentially fully polarized ($>99.9\%$). However, the reflected beam has a polarization leakage from the opposite channel between 1-3% depending on wavelength. This causes the presence of residual light in arm 2 even for crossed polarizer configuration (Figure 6) and a loss in fractional polarimetric efficiency of arm 2 relative to arm 1 of up to 5.5% which can be seen in Figure 7.

The leakage l can be measured with CCD 2 if fully polarized light is rotated in front of the beam-splitter. Then l is the ratio between the intensity of the light parallel (minimum of arm 2) and perpendicular (maximum of arm 2) to the transmission arm of the beam-splitter (corrected for charge leakage from open to covered rows, see section 6.3):

$$l = \frac{I_{par}}{I_{per}} \quad (1)$$

Finally, the fractional polarimetric signal $(Q/I)_0$ of the reflected beam is reduced according to

$$\left(\frac{Q}{I}\right)_m = \left(\frac{Q}{I}\right)_0 \cdot \frac{1-l}{1+l} \quad (2)$$

whereas the leakage l has no effect on the fractional polarization of the transmission beam.

5.2 Polarimetric properties of the calibration optics

Since ZIMPOL is optimized for the measurement of linear polarization the most important components for the polarimetric calibration are the linear polarizer and HWPZ while the quarter-wave plate and the circular polarizer are of minor importance.

- Linear polarizer:**
 The achromatic dichroic glass polarizer is made of structured absorptive nanoparticles. It provides an excellent contrast of better than 1:1000 between 600-900 nm which is reduced to about 1:100 between 500-600 nm.
- Quarter-wave plate:**
 For the measurement of instrumental circular polarization ZIMPOL is equipped with an achromatic quarter-wave plate made out of MgF_2 and quartz. The retardance error for the range of 500-900 nm is less than $\pm 6\%$ with a similar wavelength dependence as HWPZ (Figure 5).
- Circular polarizer:**
 The circular polarizer is a combination of a linear polarizer with the fast axis at $45^\circ (\pm 0.5^\circ)$ followed by a quarter-wave plate with the fast axis at 0° . Both components are of the same type as the individual components described above. Since the quarter-wave plate is not perfectly achromatic the circular polarizer has a small leakage of linear polarization of several percent.
- HWPZ**
 Like the quarter-wave plate the achromatic HWPZ is made out of MgF_2 and quartz and it is designed for the range of 500-900 nm. Figure 5 shows the retardance as function of wavelength. The retardance error is less than $\pm 6\%$.

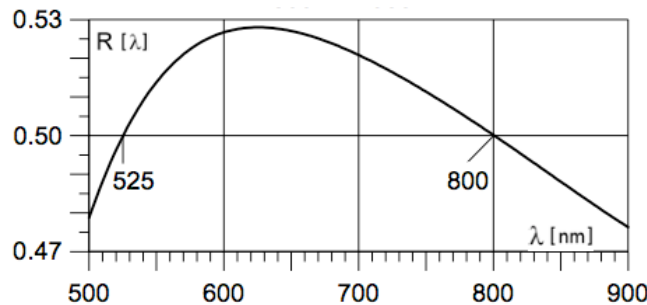


Figure 5 HWPZ retardance curve provided by the manufacturer (Bernhard Halle Nachfolger GmbH).

5.3 Alignment of the polarization axis

The reference orientation for the polarimetric alignment is given by the polarizing beam-splitter of ZIMPOL and the transmission beam (CCD 1) corresponds to linear polarization parallel to the ZIMPOL bench. Hence the polarization of the reflected beam (CCD 2) is oriented perpendicular to the bench.

All the calibration components of ZIMPOL (including HWPZ) have been mounted and aligned during subsystem testing at ASTRON in Dwingeloo^[12]. We consider here only the alignment of the rotational position of the optical axis which is of importance for the polarimetric aspects of ZIMPOL / SPHERE. The linear polarizer is aligned parallel to the bench and the quarter-wave plate is mounted with the fast axis rotated by 45 degrees. Therefore, circular polarized light will be transformed into linear polarized light in Q direction (and vice versa). The orientation of the circular polarizer is such that the polarization axis of its linear polarizer is at 45°. Therefore, the residual linearly polarized light due to the quarter-wave plate retardance error is oriented in U direction ($\pm 45^\circ$) where ZIMPOL is not sensitive.

For the initial alignment an external rotatable polarizing beam-splitter of the same type as the internal one was placed in front of ZIMPOL. For all components the alignment principle was similar. Discrete measurement scans were taken by rotating HWPZ or the external polarizer respectively to determine the amount of extinction due to crossed polarizers. Then, a sine curve is fitted to the data points. The alignment was carried out using the ZIMPOL narrow R filter (655/60nm, see Table 4) in FW1 and FW2 respectively. Table 1 gives a summary of the corresponding scan configurations and the accuracy of the final alignment. An example of such a scan is shown in Figure 6 for the measurement of the HWPZ zero-point. In the reflection arm (CCD 2) one can also see that the flux is always > 0 which is due to the leakage of the beam-splitter of light with opposite polarization (see section 5.1).

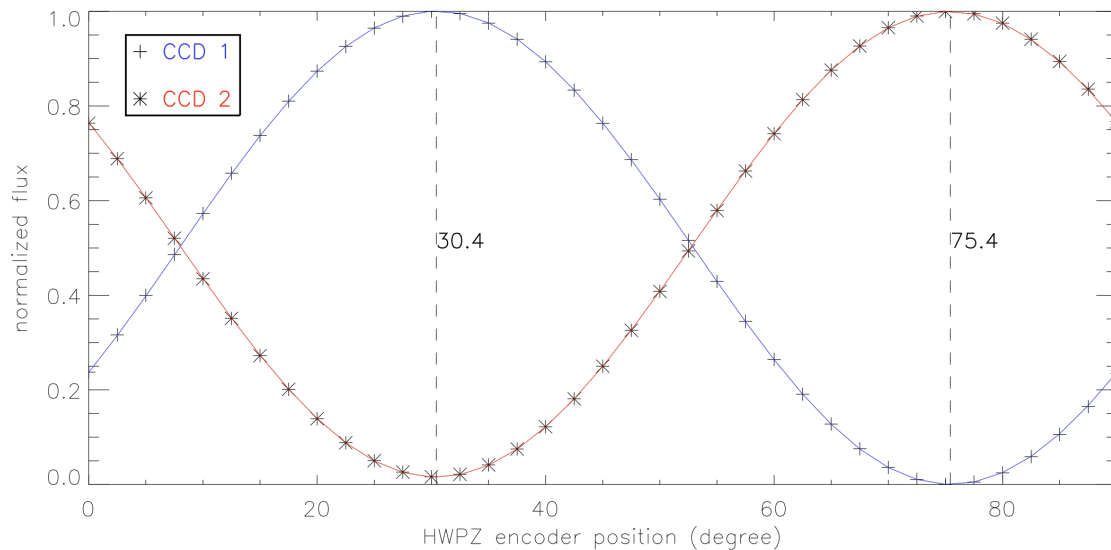


Figure 6 Alignment scan for HWPZ. The vertical dashed lines indicate the positions of the minima and maxima ($\pm 0.1^\circ$). According to this result the real zero-point of HWPZ corresponds to the hardware encoder angle 75.4° .

Table 1 Configurations of the optical polarization components for the alignment scans rotating either the external beam-splitter or HWPZ. The last two columns give the final orientations and uncertainties ($0^\circ =$ perpendicular to the bench).

component to align	external BS	FW0	HWPZ	orientation	uncertainty
external beam-splitter	0° - 180° (5°)	open	out	-	$\pm 0.2^\circ$
linear polarizer	0° - 180° (5°)	linear polarizer	out	90°	$\pm 0.5^\circ$
HWPZ	-	linear polarizer	0° - 180° (5°)	0°	$\pm 0.5^\circ$
Quarter-wave plate	0° - 180° (5°)	quarter-wave plate	22.5°	45°	$\pm 2.5^\circ$
Circular polarizer	0° - 180° (5°)	circular polarizer	out	45°	$\pm 2.5^\circ$

The final alignment for the linear polarizer and HWPZ is better than $\pm 0.5^\circ$ which is very well within specifications. This should allow an absolute polarimetric calibration of ZIMPOL on-sky measurements with an accuracy of about $\pm 0.1\%$.

For the quarter-wave plate and the circular polarizer the alignment accuracy is about $\pm 2.5^\circ$. This is also acceptable because the system is optimized for measuring linear polarization and these two components are mainly used for the assessment of cross-talk effects between linear and circular polarization. Hence the alignment requirements for these two components are less tight.

6. TESTS AND PERFORMANCE OF THE FLC-MODULATOR PACKAGE

6.1 Definitions: Polarimetric efficiency and cross-talks

We define the following expressions to describe the performance of the FLC-modulator package:

- **(fractional) Polarimetric efficiency ϵ :** $\pm Q/I \rightarrow \pm \epsilon * Q/I$
The measured polarization signal in Q-direction (parallel to beam-splitter) for incoming $\pm Q$ -polarization.
- **(fractional) Cross-talks c_{UQ} , c_{VQ} :** $\pm U/I \rightarrow \pm c_{UQ} * Q/I$ and $\pm V/I \rightarrow \pm c_{VQ} * Q/I$
The measured polarization signal in Q-direction for incoming $\pm U$ -polarization or $\pm V$ -polarization.

The cross-talks and the efficiency are wavelength and modulation frequency dependent and to a lesser extent affected by aging effects. Hence cross-talk and efficiency measurements are an essential part of the calibration and monitoring program of ZIMPOL. Table 2 gives an overview of the corresponding configurations of the FW0 components and HWPZ to produce the efficiency and cross-talk measurements. The polarization signal Q/I is calculated by

$$\frac{Q}{I} = \frac{(I_0 - I_{90})}{(I_0 + I_{90})} \quad (3)$$

where I_0 and I_{90} correspond to the detector averaged intensities of the two modulation states.

A perfect polarimetric system measures the polarization signal with $\epsilon_{\text{tot}} = 1$. In SPHERE/ZIMPOL the efficiency is reduced by different optical effects and detector effects.

Optical effects:

- The calibration components are not perfect but have small achromatic residuals. In addition some slight misalignments of the reference axes of the FLC, HWPZ and the beam-splitter lead to slightly different absolute values of the measured percentage polarization if the sign of the incoming Stokes vector is changed. One measured signal is up to 3% higher than the other. Therefore we combine both signals to:

$$\frac{Q}{I} = \frac{1}{2} \cdot \left(\left(\frac{Q}{I} \right)_{\text{plus}} - \left(\frac{Q}{I} \right)_{\text{minus}} \right) \quad (4)$$

- The switch time between the two opposite states of the photo-electric modulator is finite and requires a time of about 50 to 80 μs .
- The optical components of the telescope and instrument introduce a small efficiency loss due to polarization cross-talks e.g. from linear to circular polarization.

Detector effects:

- The charge-shifting demodulation time is finite and some synchronization errors between modulator and detector may cause a loss in efficiency.
- Static charge and light leakage on the masked CCDs from the illuminated pixel rows to the covered buffer rows. We denote this effect as detector efficiency (see below).

The detector effects and the modulation-demodulation effects are discussed in detail in Schmid et al. (2012)^[9] and a theoretical description of the static optical effects using the Mueller matrix formalism is described in Gisler et al. (2004)^[7]. In the following two sections we describe the main properties of the modulator, the switch time and the switch angle, and we show how to separate the modulator effects from the main detector effects. Finally, we derive the wavelength dependence of the polarization efficiency and the polarization cross-talks of the modulator package and discuss the impact of the polarimetric alignment and chromatic residuals of the calibration optics.

Table 2 Overview of the configurations to measure the polarimetric efficiency and cross-talks (*→Q) of ZIMPOL. The last column gives an example of the values for camera 1 in fast polarimetry mode using the narrow R filter. See Table 4 for the filter width.

	FW0	HWPZ	FastPol / Cam1 / nR [%]
+Q → Q	linear polarizer	in / 0°	83.2
-Q → Q	linear polarizer	in / 45°	-85.7
+U → Q	linear polarizer	in / 22.5°	5.7
-U → Q	linear polarizer	in / -22.5°	-3.7
+V → Q	circular polarizer	out	-6.7
-V → Q	circular polarizer	in / 0°	6.9

6.2 Basic properties of the ferro-electric liquid crystal modulator

For the polarimetric modulation SPHERE/ZIMPOL uses a ferro-electric liquid crystal (FLC) modulator. The fast optical axis of the FLC retardance is switched between two angles, 0° and approximately 45°, with a cycle frequency of 967 Hz in fast modulation mode and 27 Hz in slow modulation mode.

Intrinsically the FLC modulator is chromatic with an exact half-wave retardance at the one nominal wavelength λ_0 only. The wavelength dependence of the retardance behaves according to $\sim 0.5 \lambda_0/\lambda$ similar to a zero-order half-wave plate. Therefore, the FLC is combined with a quartz zero-order half-wave plate (0-HWP) with a special combination of orientations of the optical axes which provides a close to achromatic modulation^[7].

The required switch time between the two modulator states is another key parameter for the efficiency of the FLC. In general the switch time is shorter for higher temperatures and higher driver voltages^[13]. In the case of the ZIMPOL FLC the driver voltage is fixed and cannot be tuned. The temperature has also an influence on the switch angle which will be significantly different from 45° for extreme temperatures^[13]. In a trade-off analysis we selected for the FLC an operation temperature of 25 °C, which provides a switch angle of 46° and a switch time of 70 μ s. Higher temperatures would allow for shorter switch times but then the switch angle is less favorable. Low temperatures < 15 °C are not acceptable because the switch time is too slow for a modulation frequency of 967 Hz.

An operation temperature of 25 °C is already quite demanding, because it is much higher than the ambient temperature of 0-15 °C expected at the VLT telescope. For this reason the FLC is heated and thermally encapsulated in a small vacuum chamber in order to have its temperature stabilized and to avoid thermal turbulence in the system. On the entrance window of the vacuum chamber the 0-HWP plate is mounted with a slight tilt with respect to the optical beam in order to avoid ghost images. An overview of the main specifications of the FLC and the 0-HWP are given in Table 3.

Table 3 FLC properties measured at ETH. All measurements have been done with the full aperture. The switch time is the measured time between 10% and 90% of the maximum intensity signal when the FLC modulator switches from one state to the other. Design wavelength means the wavelength with exactly $\lambda/2$ retardation. More details are given in the text.

	FLC	0-HWP
Switch angle	45.8° ± 0.5°	-
Switch time	75 μ s	-
Design wavelength	662.3 nm	689.5 nm
T operation range	25 °C	0 – 15 °C
Position angle fast axis	-26.3°	64.4°

Of course, instead of minimizing the switching time one can also decrease the modulation frequency which will reduce the proportional switching overhead with respect to the well defined modulation states. However, since one of the key characteristics of ZIMPOL is a modulation faster than the seeing variations the frequency cannot arbitrarily be reduced. Taking this into account ZIMPOL provides a fast modulation mode with a frequency of 967 Hz suited for high precision polarimetry of bright targets < 4-7 mag and a slow modulation mode at 27 Hz for faint targets and observations in narrow-band filters or further out in the PSF.

6.3 FLC effects vs. Detector Effects

The wavelength dependent modulation-demodulation efficiency of ZIMPOL is mainly caused by the switching efficiency of the FLC modulator which in turn is dependent on the modulation frequency. However, charge diffusion from the open into the masked pixel rows further diminishes the polarimetric efficiency of the system^[9]. We refer to this effect as the detector efficiency. Finally, when the system is running without the fast shutter at the entrance of the ZIMPOL optical path a third effect arises which is especially important for short integration times. If the shutter is off the detector is still exposed to light during the frame transfer for read-out. For a flatfield illumination this leads to an additional intensity uniformly smeared over all pixels. This is called the frame transfer smearing (FTS).

Therefore, by introducing the parameter τ , i.e. the ratio between the detector integration time (DIT) and the frame transfer time, the pure FLC polarization signal $(Q/I)_{FLC}$ is calculated by

$$\left(\frac{Q}{I}\right)_m = \left(\frac{Q}{I}\right)_{FLC} \cdot \frac{2\delta - 1}{\frac{1}{\tau} + 1} \quad (5)$$

with δ denoting the detector efficiency. Depending on the frame transfer time the FTS can easily cause a DIT-dependent deviation in modulation-demodulation efficiency of a few percent whereas the detector efficiency leads to a constant offset of around 10%.

6.4 Actual performance of the FLC modulator

The theoretical polarization efficiency and cross-talks of the modulator package can be calculated with the Stokes vector and Mueller matrix formalism^[7]. Figure 4 shows the results of measurements in fast and slow modulation mode and compares them with the expected values from simulations assuming an instant switching time. The data have been corrected for detector efficiency and charge transfer smearing and were reduced using the SPHERE DRH-software^[14] (Data Reduction and Handling) for basic data reduction (i.e. dark and bias subtraction, calculation of Stokes parameters) in combination with some of our own IDL scripts to further analyse the data. The polarization was calculated as the mean over a 490x490 image area (complete area 512x512) cutting away 10 pixels on each border. Note that the image is not flat but it has a gradient of about 6% from down/left to up/right arising from the microlens array on the CCD mask.

In slow modulation mode the polarimetric efficiency is between 96-98% for all polarimetric filters. Hence for the slow modulation mode the effect of the switching efficiency is negligible and the theoretical values for an instant switch time are achieved. Because of the growing impact of the finite switch time about 7.5% is lost in efficiency for the fast modulation mode. In addition up to 5.5% are lost in the reflection arm both for fast and slow modulation equally because of polarimetric leakage from the opposite polarization direction (see section 5.1).

To assess the impact of the polarimetric efficiency and the cross-talks on the final polarimetric calibration let us assume an ideal HWPZ and only consider ε and c_{uq} i.e. the efficiency and the $U \rightarrow Q$ cross-talk respectively. Therefore, the measured polarization p_m will become:

$$p_m = \sqrt{\varepsilon^2 + c_{uq}^2} \cdot p_0 \quad (6)$$

To first order we only calibrate for the efficiency and we get:

$$\tilde{p}_0 \approx \sqrt{1 + \frac{c_{uq}^2}{\varepsilon^2}} \cdot p_0 \approx (1 + 0.02) \cdot p_0 \quad (7)$$

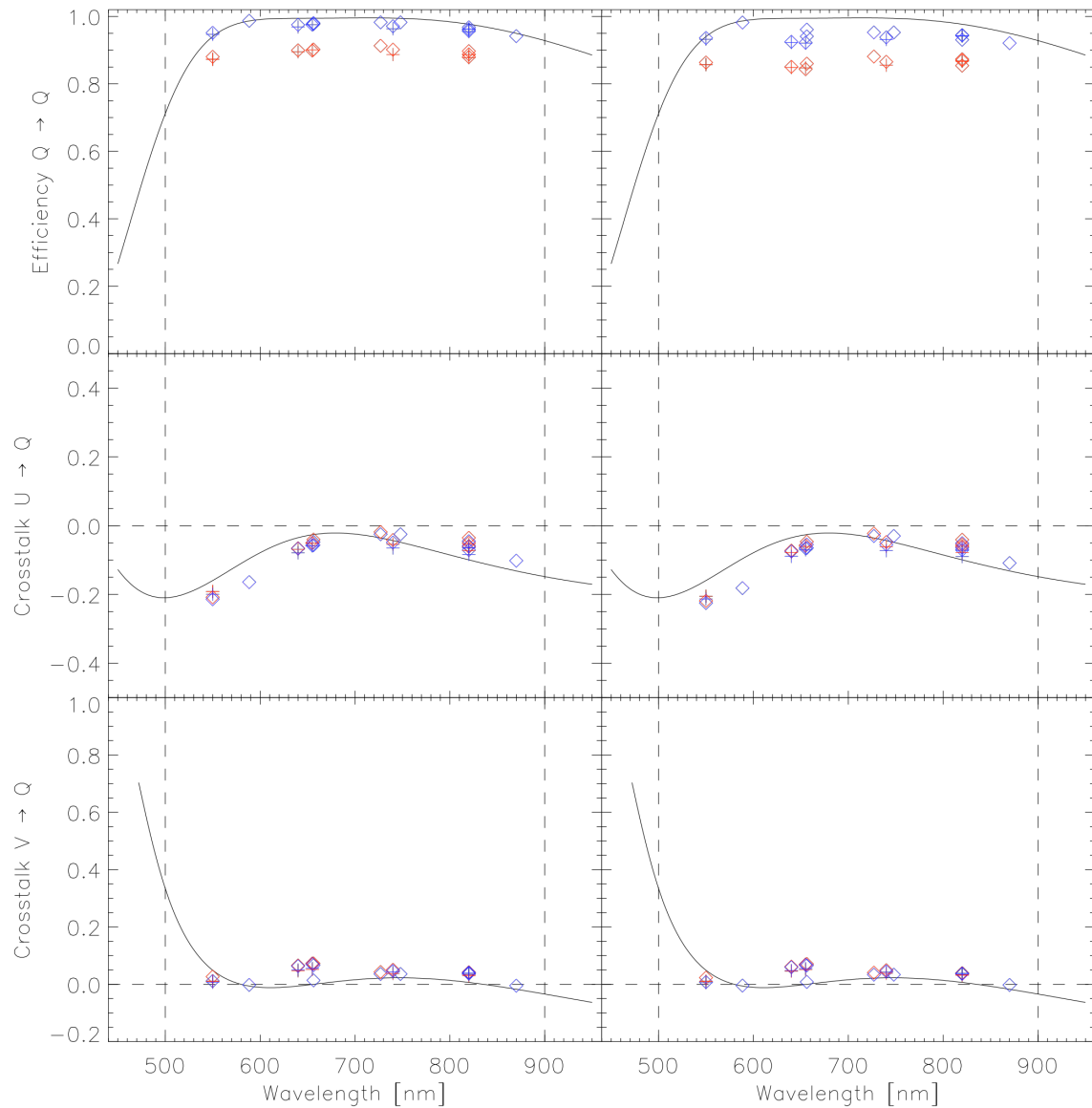


Figure 7 Wavelength dependent efficiency and cross-talks measured at ASTRON (diamonds) and IPAG (crosses) in the transmission (left) and reflection (right) arm. The solid line is the theoretical value for an instant FLC switching time. Blue data points correspond to slow modulation mode and red data points to fast modulation mode. Only the center wavelengths are indicated. See Table 4 for the filter widths. The difference between fast and slow modulation is about 7.5% for both arms and the difference of about 5.5% between transmission and reflection arms is due to a polarization leakage of the beam-splitter. More explanations are given in the text.

whereas we adopted the V-band values from Table 4 (i.e. the values with the highest $U \rightarrow Q$ cross-talk). One can see that to first order the $U \rightarrow Q$ cross-talks are negligible and we can already calibrate the polarization to a level better than 0.02^*p . The analysis for the impact of the cross-talk $V \rightarrow Q$ is similar.

The uncertainty of the efficiency $\Delta\epsilon$, i.e. the difference of the results for incoming $\pm Q$ polarization due to slight optical misalignments, is typically around $\pm 1.5\%$ (except in the V-band: $\pm 2.5\%$). Therefore, the uncertainty for the efficiency corrected polarization signal is already very small. For example:

$$\left(\frac{\tilde{Q}}{I}\right)_0 = \left(1 \pm \frac{\Delta\varepsilon}{\varepsilon}\right) \cdot \left(\frac{Q}{I}\right)_0 \approx (1 \pm 0.015) \cdot \left(\frac{Q}{I}\right)_0 \quad (8)$$

for $\varepsilon = 0.95 \pm 0.015$. In the final polarimetric calibration it is foreseen to take also the effects of HWPZ into account to push the uncertainty below $(\pm 0.01) \cdot (Q/I)$.

Table 4 Results for the fractional polarization efficiency (Q→Q) and cross-talks for the slow modulation mode in the transmission arm (not affected by beam-splitter leakage). According to equation 5 the data has been corrected with the detector efficiency δ and the FTS. Indicated in blue are the filters that are not intended for polarimetry but only for imaging. The uncertainty of the efficiency, i.e. the difference of the results for incoming $\pm Q$ polarization, is typically about $\pm 1.5\%$ (except in the V-band where it is $\pm 2.5\%$).

Filter names	λ / width [nm]	δ [%]	Q → Q [%]	U → Q [%]	V → Q [%]
V-band	550 / 80	95.9	95.1	-21.3	1.1
HeI / NaI	588.5 / 5	96.5	98.7	-16.4	-0.2
R-band	640 / 150	97.0	97.5	-6.7	6.3
Narrow R	655 / 60	97.0	97.6	-5.7	7.1
H-alpha broad	656.3 / 5	96.9	98.0	-4.8	6.7
H-alpha cont.	656.3 / 1	97.2	97.8	-5.7	1.4
Very broad band	740 / 290	97.4	97.1	-4.9	4.7
Cont	748 / 20	97.8	98.2	-2.5	3.6
Narrow I	820 / 80	97.5	96.1	-5.9	3.9
I-band	820 / 150	97.7	96.8	-4.5	3.8
Cont	820 / 20	97.6	95.7	-7.1	4.1
I-long	870 / 60	96.0	94.2	-10.2	-0.5

7. CONCLUSION

This paper outlines the basic polarimetric measuring and calibration concept for the ZIMPOL / SPHERE imaging polarimeter and describes in detail the implemented FLC polarization modulator and polarimetric calibration components. ZIMPOL is based on a fast modulation-demodulation technique which requires for the detection of faint sources a broad-band opto-electric polarization modulator. The main polarimetric challenge for this modulator is a high polarimetric efficiency over a broad wavelength range for the search of faint sources like extra-solar planets. For high S/N measurements of bright targets an accurate calibration of the wavelength dependent polarimetric properties is important.

We assess first the alignment precision of the internal calibration components which needs to be accurately known for the polarimetric characterization and calibration of ZIMPOL. Using the internal calibrators we then derive the wavelength dependence of the polarization efficiency and the polarization cross-talks of the modulator package. The analysis separates the effects of the modulator package from those of the demodulating detector. Our study shows that the polarimetric modulation of the used modulator is within specifications and our characterization of its properties is sufficiently accurate for the polarimetric calibration of future data. The presented data will also serve as a starting point for instrument checks after reassembly of the SPHERE instrument at the telescope and for the long-term monitoring of the polarimetric characteristics of ZIMPOL / SPHERE.

High performance tests of the entire ZIMPOL subsystem also showed that the used ZIMPOL polarization modulator package performs close to expectations^[11]. The polarimetric properties are very good but a small beam shift effect was noticed in high-contrast performance tests. This effect introduces a slight beam shift of a small fraction of a detector pixel between the two modulation stages which currently dominates the systematic residuals in the differential image in

high performance tests of bright point sources. This problem may be solved with post-processing or with the half-wave plate switch technique using accurate point source centering with the AO system. The polarimetric characterization of ZIMPOL and the gained information for the calibration of future data is not affected by this problem unless the polarization modulator must be replaced. Then new measurements of the modulator properties as presented in this work need to be carried out.

REFERENCES

- [1] Beuzit, J.L., Feldt, M., Dohlen, K., Mouillet, D., Puget, P. and SPHERE Consortium, "SPHERE: a Planet Finder instrument for the VLT." ESO Messenger 125, 92
- [2] Beuzit, J.L., Feldt, M., Dohlen, K., Mouillet, D., Puget, P., Wildi, F.P., and SPHERE Consortium, "SPHERE: a Planet Finder instrument for the VLT," Proc. of SPIE Vol. 7014, Paper 701418 (2008)
- [3] Schmid, H.M., Beuzit, J.L., Feldt, M., Gisler, D., Gratton, R., Henning et al., "Search and investigation of extra-solar planets with polarimetry," IAU Coll. 200, 165–170 (2006)
- [4] Povel, H.P., Aebersold, F., and Stenflo, J., "Charge-coupled device image sensor as a demodulator in a 2-D polarimeter with a piezoelectric modulator," Appl. Opt. 29, 1186 (1990)
- [5] Povel, H.P., "Imaging Stokes polarimetry with piezoelectric modulators and charge-coupled-device image sensors," Optical Engineering 34, 1870 (1995)
- [6] Stenflo, J.O., Keller, C.U., "New Window for Spectroscopy," Nature 382, 558 (1996)
- [7] Gisler, D., Schmid, H.M., Thalmann, C., Povel, H.P., Stenflo, J.O., Joos, F., et al., "CHEOPS/ZIMPOL: a VLT instrument study for the polarimetric search of scattered light from extrasolar planets," Proc. of SPIE Vol. 5492, 463-474 (2004)
- [8] Thalmann, C., Schmid, H.M., Boccaletti, A., Mouillet, D., Dohlen, K., Roelfsema, R., Carbillet, M., et al., "SPHERE ZIMPOL: overview and performance simulation," Proc. of SPIE Vol. 7014, 70143F (2008)
- [9] Schmid, H.M., Downing, M., Roelfsema, R., Bazzon, A., Gisler, Pragt, J., Cumani, C., et al., "Tests of the demodulating CCDs for the SPHERE/ZIMPOL imaging polarimeter," Proc. of SPIE Vol. 8446, submitted (2012)
- [10] Joos, F., [Polarimetry of gas planets], Ph.D. Thesis, Diss ETH No. 17051 (2007)
- [11] Roelfsema, R., Gisler, D., Pragt, J., Schmid, H.M., Bazzon A., Dominik C., et al., "The ZIMPOL high contrast imaging polarimeter for SPHERE: sub-system test results," Proc. of SPIE Vol. 8151, 81510N (2011)
- [12] Pragt, J., Roelfsema, R., Gisler, D., Wildi, F., Schmid, H.M., Rigal, F. et al., "Alignment of the SPHERE-ZIMPOL polarimeter," Proc. of SPIE Vol. 8446, submitted (2012)
- [13] Gisler, D., [Instrumentierung für hochpräzise Vektorpolarimetrie in der Astronomie], Ph.D. Thesis, Diss ETH No. 16110 (2005)
- [14] Pavlov, A., Möller-Nilsson, O., Feldt, M., Henning, T., "SPHERE data reduction and handling system: overview, project status, and development," Proc. of SPIE Vol. 7019, 701939 (2008)